Combustion Chambers for Natural Gas SI Engines Part 2: Combustion and Emissions

Olsson, Krister; Johansson, Bengt

Published in:
SAE Transactions, Journal of Engines

1995

SAE TECHNICAL
PAPER SERIES

950517

Combustion Chambers for Natural Gas SI Engines Part 2: Combustion and Emissions

Krister Olsson and Bengt Johansson
Lund Institute of Technology

The Engineering Society
For Advancing Mobility
Land Sea Air and Space®
INTERNATIONAL

International Congress and Exposition
Detroit, Michigan
February 27 - March 2, 1995

400 Commonwealth Drive, Warrendale, PA 15096-0001 U.S.A. Tel: (412)776-4841 Fax:(412)776-5760

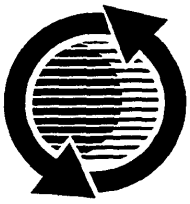

ISSN 0148-7191

Printed in USA 90-1203D/PG

950517

Combustion Chambers for Natural Gas SI Engines Part 2: Combustion and Emissions

Krister Olsson and Bengt Johansson
Lund Institute of Technology

ABSTRACT

The objective of this paper is to investigate how the combustion chamber design will influence combustion parameters and emissions in a natural gas SI engine.

Ten different geometries were tried on a converted Volvo TD102 engine. For the different combustion chambers emissions and the pressure in the cylinder have been measured. The pressure in the cylinder was then used in a one-zone heat-release model to get different combustion parameters. The engine was operated unthrottled at 1200 rpm with different values of air/fuel ratio and EGR. The air/fuel ratio was varied from stoichiometric to lean limit. EGR values from 0 to 30% at stoichiometric air/fuel ratio were used.

The results show a remarkably large difference in the rate of combustion between the chambers. The cycle-to-cycle variations are fairly independent of combustion chamber design as long as there is some squish area and the air and the natural gas are well mixed.

Geometries that give the fastest combustion give the highest NO_x values at λ=1.2, but at λ>1.5, which is normally designated lean-burn, the differences are smaller. The lowest NO_x values for lean burn were obtained with the geometries that gives fast combustion.

The HC emissions display some correlation between high combustion rate and low levels of HC emissions, but combustion chambers with dead zones and large total combustion chamber areas give higher HC contents than the combustion rate alone would indicate.

Indicated efficiency is reduced for combustion chambers with a large total combustion chamber surface area and thus large heat losses. High levels of turbulence also tend to reduce the efficiency for the same reason.

INTRODUCTION

Most natural gas commercial vehicles are using converted relatively large diesel engines. The combustion chamber in these engines is most commonly located in the piston crown and a flat cylinder head is used. The inlet port of these engines often generates a highly swirling gas motion to enhance the diesel combustion process. In the conversion to spark ignition operation, the original inlet port is most often used. The original combustion chamber is, however, not directly suitable for SI operation as the compression ratio often is too high and the flow structure is optimised for spray combustion rather than the flame propagation of a SI engine. But the question is how the piston crown modification should be performed to get the minimum amounts of emissions and at the same time a high thermal efficiency.

To get an indication of the importance of the combustion chamber geometry ten different geometries were manufactured for a Volvo TD102 1.6 litre single cylinder engine. For these geometries, the in-cylinder flow, combustion and the emission characteristics were measured. In the previous paper the in cylinder flow measurements were presented together with combustion parameters when the engine operated at λ=1.5. In that paper was found that the rate of combustion changed significantly for the chambers.

In the present paper the emissions as well as the combustion parameters will be presented with the engine operating with air/fuel-ratios from stoichiometric to the lean limit as well as with different amounts of EGR. The combustion events were measured by using the cylinder pressure and a simple heat-release analysis. The indicated mean effective pressure (IMEP) and the duration of 0-10% and 10-90% heat-released were registered among other parameters.

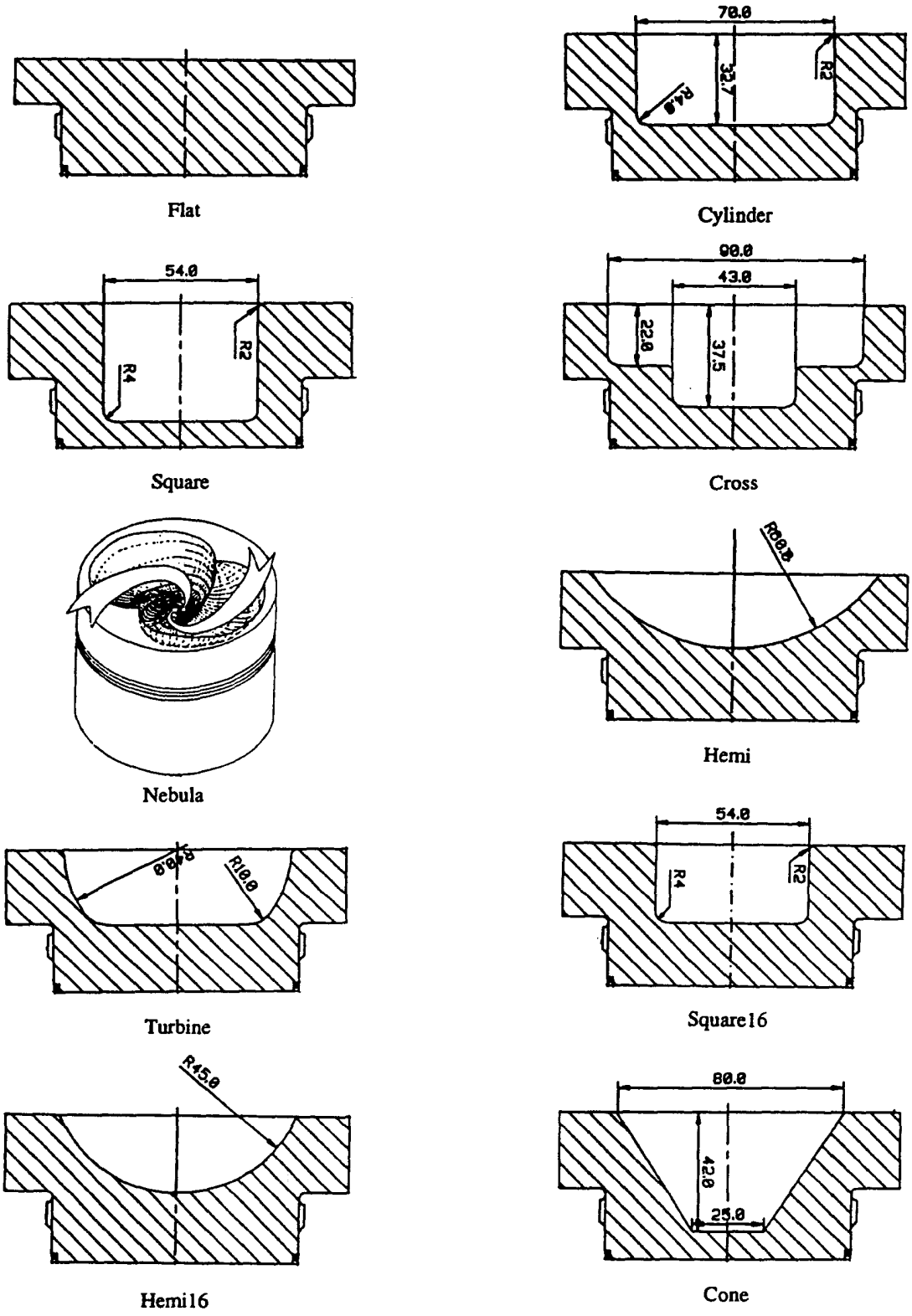

Figure 1: Geometry of the combustion chambers used.

The different combustion duration for the combustion chambers would be expected to produce different levels of NO_x emissions as the maximum pressure and hence temperature would increase for a fast combustion chamber. The different surface area for the combustion chambers would he expected to influence the levels of HC emissions.

COMBUSTION CHAMBERS

The combustion chambers used to study the effect of chamber geometry on emissions and combustion rate were designed in a cut and try fashion. To make it easy to change combustion chamber geometry a two-piece piston was developed for a 1-cylinder experimental engine. The lower part of the piston consists of a standard piston that has been cut above the upper piston-ring groove and then threaded internally. Upper parts with different combustion chamber geometries have then been made. The advantage of this piston is that one only needs to remove the cylinder head when changing the geometry of the combustion chamber. The disadvantage is that it is not possible with absolute certainty to compare results with those obtained using a single-piece piston, as efficiency is affected by the different heat transfer characteristics of the pistons.

The nominal compression ratio for most chambers was set to 12:1. This ratio corresponds well to the ratio used in present natural gas heavy duty engines [1],[2],[3]. Three geometries were, however, designed with a higher ratio to study the effect of compression ratio. The main geometric data for the selected combustion chambers are presented in figure 1 and table 1. More detailed descriptions of the geometries can be found in Part 1.

Table 1: Geometry of the used combustion chambers

Comb. Chamber	*Squish/ Bore*	*Area/ Bore*	*Bowl depth*	*Bowl diam.*
			mm	*mm*
Flat	*0*	*1.3572*	*"10.7"*	*-*
Cylinder	*0.66*	*1.5709*	*32.7*	*D=70*
Square	*0.74*	*1.7297*	*42.5*	*54×54*
Cross	*0.42*	*1.7830*	*22,37*	*see fig 1*
Nebula	*0.25*	*-*	*28.5*	*-*
Hemi	*0.30*	*1.2631*	*28.5*	*R=60*
Turbine	*0.55*	*1.4069*	*25*	*D=80*
Square 16	*0.74*	*1.4740*	*29.1*	*54×54*
Hemi 16	*0.55*	*1.2257*	*29*	*R=45*
Cone	*0.55*	*1.2886*	*42*	*D=80, d=25*

EXPERIMENTAL APPARATUS

The engine- The measurements were made in a single cylinder engine based on a six-cylinder Volvo TD 102 diesel engine. Its main geometric properties are shown in table 2.

Table 2: Geometric properties of the engine.

Displaced volume	*1600*	*cm^3*
Bore	*120.65*	*mm*
Stroke	*140*	*mm*
Connection rod	*260*	*mm*
Exhaust valve open	*39 CAD BBDC*	
Exhaust valve close	*4 CAD ATDC*	
Inlet valve open	*2 CAD BTDC*	
Inlet valve close	*42 CAD ABDC*	

The exhaust gas analysis system- For the exhaust gas measurements a 'P7450 Automotive Exhaust Gas Analysis System' from Cusson was used. The exhaust gas was continuously sampled from the exhaust gas stream via a heated sample line to a heated distribution module. The heated distribution module contains sample pump and filters. Total hydrocarbons were analysed in a heated flame ionisation detector that is fed via a heated line from the distribution module. Oxides of nitrogen were analysed by a chemiluminescent analyser with a heated capillary module that was also fed via a heated line from the distribution module. Carbon dioxide and carbon monoxide were measured by non-dispersive infrared analysers while oxygen was measured by a paramagnetic analyser. Before entering these analysers the sample was cooled to remove excess water vapour, and filtered. See figure 2.

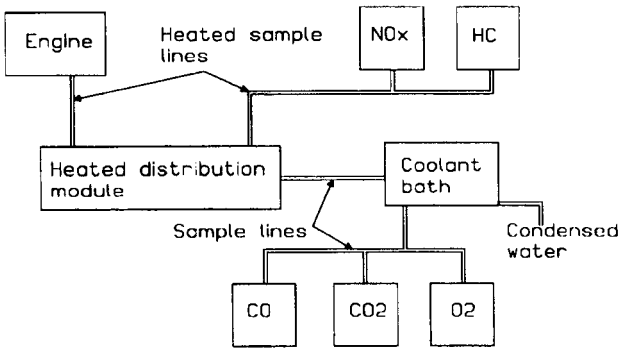

Figure 2: The exhaust gas analysis system. [4]

Each analyser was calibrated with appropriate calibration gas from bottles before and during every measurement. More details about the analysers can be found in [4]. In order to be able to evaluate the percentage

of exhaust gas recycled (EGR), the oxygen fraction in the inlet mixture was measured. This O_2 analyser was also a paramagnetic analyser.

The Pressure measurement system- The pressure in the cylinder was measured with a AVL QC42 piezo-electric transducer connected to a Kistler 5001 charge amplifier. The charge amplifier voltage output was connected to a 486/66 PC with a Data Translation DT2823 100 kHz 16-bit A/D-card. A more detailed description can be found in [5].

The Flow measurement system- The air flow was measured with a Bronkhorst mass flow meter F-106A-HC. The natural gas flow was measured with a Bronkhorst mass flow meter F-106B-HD.

The control system- The ignition timing was controlled with a PC-controlled system. Triggering signals to the pressure-system were also included in this system. Input signals to the control system were a sync-pulse (1 pulse per 2 revs), a TDC pulse (1 pulse per rev) and a crank angle-pulse (5 pulses per crank angle degree, CAD).

OPERATING CONDITIONS

The engine was run on natural gas that was fed to the engine through two pulse width-modulated solenoid valves.

The valves were controlled by an Intelligent Control IC5460 engine management system. To get a homogenous charge the mixing length from the solenoid valves to the engine was 3 m with a 16 litre mixing tank in the middle. The influence of different amounts of fuel and air into the engine from cycle to cycle is therefore reduced.

During all emissions and cylinder pressure measurements, the engine was run at 1200 rpm and no throttling was applied.

DATA REDUCTION

One-zone heat-release model- To extract information on the flame development, a cycle-resolved heat-release calculation was performed. In the computations Wochnis heat transfer model [6] was applied and the ratio of specific heats was assumed to have a linear dependence on temperature. Further details concerning the heat-release calculation have been described elsewhere [5].

Relative air/fuel ratio- To evaluate emission levels and compare them under different circumstances, the following formulas were used to calculate the relative air/fuel ratio, λ [4].

λ is defined as follows:

$$\lambda = \frac{\left(\frac{A}{F}\right)_{actual}}{\left(\frac{A}{F}\right)_{stoichiometric}}$$

where A/F is air fuel ratio by mass

Global combustion reaction is assumed to be:

$$C_nH_mO_r + \lambda \cdot n_{o_2} \cdot (O_2 + 3.773 \cdot N_2) \Rightarrow$$

$$n_p \cdot (\tilde{x}_{CH}C_aH_b + \tilde{x}_{co}CO + \tilde{x}_{co_2}CO_2 + \tilde{x}_{o_2}O_2$$

$$+ \tilde{x}_{N_2}N_2 + \tilde{x}_{NO}NO + \tilde{x}_{NO_2}NO_2 + \tilde{x}_{H_2O}H_2O + \tilde{x}_{H_2}H_2)$$

where $n_{o_2} = n + \frac{m}{4} - \frac{r}{2}$

λ is calculated as follows:

$$\lambda = \frac{n_p \cdot (\tilde{x}_{H_2O} + \tilde{x}_{NO} + 2 \cdot \tilde{x}_{NO_2})}{2 \cdot n_{o_2}}$$

$$+ \frac{n_p \cdot (1 - \tilde{x}_{H2O}) \cdot \left(\tilde{x}^*_{CO_2} + 2 \cdot \tilde{x}^*_{O_2}\right)}{2 \cdot n_{O_2}}$$

where

$$\tilde{x}_{H_2O_2} = \frac{m \cdot \left(\tilde{x}^*_{CO} + \tilde{x}^*_{CO_2}\right)}{2 \cdot n \cdot \left[1 + \frac{\tilde{x}^*_{CO}}{K \cdot \tilde{x}^*_{CO_2}} + \frac{m}{2 \cdot n} \cdot \left(\tilde{x}^*_{CO} + \tilde{x}^*_{CO_2}\right)\right]}$$

and

$$n_p = \frac{n}{\tilde{x}_{CH} + (1 - \tilde{x}_{H_2O}) \cdot \left(\tilde{x}^*_{CO} + \tilde{x}^*_{CO_2}\right)}$$

The * denote dry exhaust gases and K is the equilibrium constant in the water gas reaction. For the calculations in this paper K = 3.5 and m/n = 3.76.

Exhaust Gas Recycled (EGR)- The EGR(%) used in this paper is defined:

$$EGR(\%) = 100 \cdot \left(\frac{\dot{m}_{EGR}}{\dot{m}_i}\right)$$

where m_{EGR} is the mass of exhaust gas recycled and m_i is the total intake mixture. The relative air/fuel ratio was maintained λ=1.0 during all the EGR measurements by the λ control option in the Intelligent Control engine management system.

The following formulas were used to calculate EGR(%):

$EGR^* = EGRflow / (Airflow + Fuelflow)$

$E = EGRflow$ has the O_2 fraction O_E

$A + F = Airflow + Fuelflow$ has the O_2 fraction O_{A+F}

$A + F + E = Airflow + Fuelflow + EGRflow$
has the O_2 fraction O_{A+F+E}

An oxygen balance gives:

$$O_{A+F} \cdot (A + F) + O_E \cdot E = O_{A+F+E} \cdot (A + F + E)$$

The equation can be rearranged to

$$(A + F) \cdot (O_{A+F} - O_{A+F+E}) = E \cdot (O_{A+F+E} - O_E)$$

and thus

$$EGR^*(\%) = 100 \cdot (O_{A+F} - O_{A+F+E}) / (O_{A+F+E} - O_E)$$

$EGR(\%)$ and EGR^* (%) are related by

$$EGR(\%) = 100 \cdot EGR^*(\%) / (100 + EGR^*(\%))$$

Lean Burn or EGR?- To get lowest possible emissions there are two possibilities. The first is to use as lean an air/fuel mixture as possible and then if necessary add an oxidising catalyst. The second is to run the engine at λ=1.0 and use as much EGR as possible and if necessary add a three-way catalyst. Both alternatives were tested and the results are presented below, first lean burn and then EGR. All measured emissions are from raw undiluted exhaust gas sampled close to the exhaust port.

LEAN BURN

Combustion- The different combustion chambers have as indicated before a large spread in the rate of heat-release. To obtain optimum performance the ignition angle θ_i has to be adjusted for the different combustion chambers and for different λ. Figure 3 below shows the ignition angle θ_i when the engine was run with MBT and with different λ. As can be seen the Square combustion chamber has the latest ignition timing for MBT. This indicates a very fast combustion rate. The Flat combustion chamber with no squish, has the earliest ignition timing.

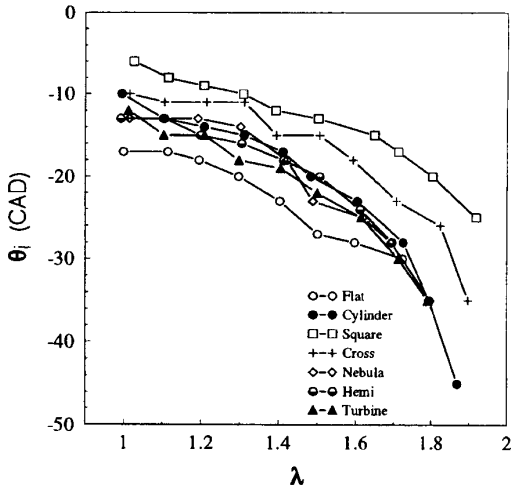

Figure 3: The crank angle position for ignition timing when different combustion chambers are used. The engine operated at MBT and 1200 rpm.

Figures 4 and 5 show the crank angle for 0 to 10% and 10 to 90% of the total heat released when the engine was run with MBT and with different λ. As can be seen it is the Square combustion chamber that has the fastest 10 to 90% combustion.

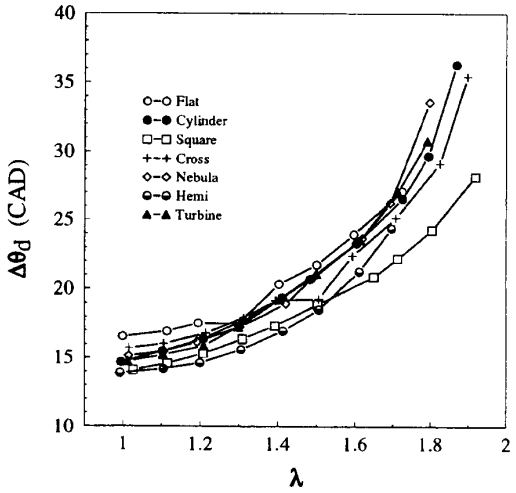

Figure 4: The flame-development angle $\Delta\theta_d$ for 0 to 10% of the total heat released when different combustion chambers are used. The engine operated at MBT and 1200 rpm.

The Flat combustion chamber, with no squish, is clearly the slowest with almost twice as long duration for the combustion. There are less differences for the 0 to 10% combustion but the combustion chambers follow more or less the same order. The exception is the Hemi that has the smallest flame development angle but the largest rapid-burn angle. The combustion 15 CAD after ignition is still mostly laminar and for the same λ the laminar flame speed is about the same. The laminar flame speed is also influenced by pressure and temperature and as different MBT values give somewhat different pressure and temperature histories can this be the reason for these small differences detected.

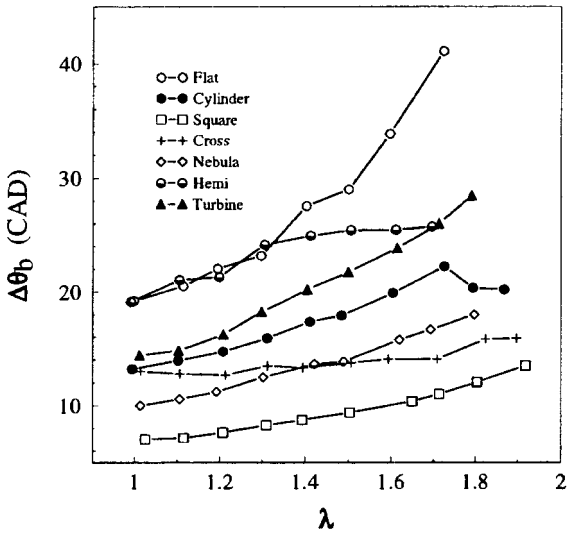

Figure 5: The rapid-burn angle $\Delta\theta_b$ for 10 to 90% of the total heat released when different combustion chambers are used. The engine operated at MBT and 1200 rpm.

Figure 5 also shows the lean limit for the different combustion chambers as the right end point of the curves. The lean limit in this paper is the highest λ-value or EGR(%) that can be used for a combustion chamber with 0% misfire during 300 continuous cycles. The reason for this rather harsh definition is that the λ-value is calculated from emission values and with misfires the values from the analysers will not be stable enough for a correct λ calculation. The Square and the Cross have the highest lean limit and the Flat and the Hemi the lowest.

Cycle-to-cycle variations- The cycle-to-cycle variations for these combustion chambers are obtained as the standard deviation of indicated mean effective pressure for 300 continuous cycles divided by the mean value (COV_{imep}). Figure 6 shows the COV_{imep} for the different combustion chambers when the engine was run with MBT and with different λ. The figure shows that with one exception COV_{imep} is almost the same for the different combustion chambers and with just a small increase for increasing λ-values up to the lean limit. The Flat combustion chamber with no squish is the only one with a COV_{imep} over 1% without any misfires and probably as a result of partial burn near the lean limit.

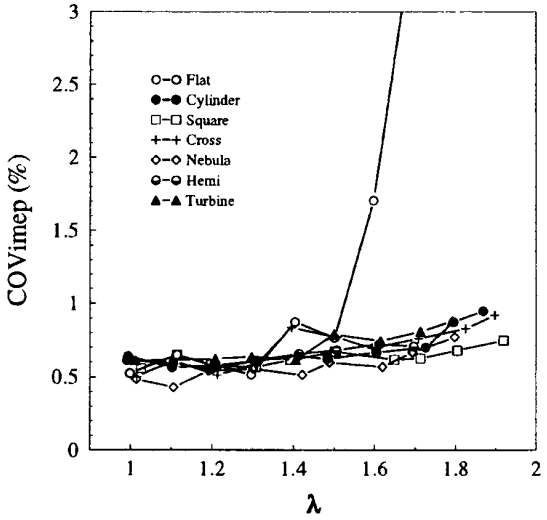

Figure 6: The COV_{imep} for different combustion chambers. The engine operated at MBT and 1200 rpm.

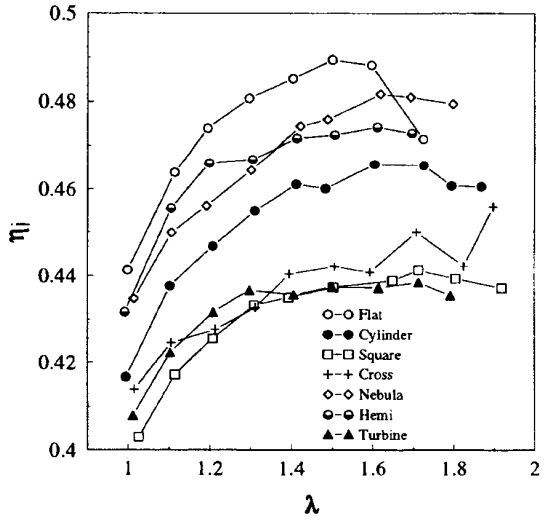

Figure 7: The indicated efficiency η_i for different combustion chambers. The engine operated at MBT and 1200 rpm.

Efficiency- The indicated efficiency, η_i, is influenced of heat losses and flow losses, both dependent on the generated turbulence. Figure 7 shows the indicated

efficiency η_i when the engine was run at MBT and with different λ The figure indicates that turbulence generating design features such as large squish areas decrease the efficiency.

Emissions- Figure 8 shows the HC emissions for the different combustion chambers. The Cross shows the highest levels of HC for all λ-values. As the Cross has the largest piston surface area this can result in a rather large contribution of HC due to wall quenching but there are also a lot of "dead" corners with slow flow rate and a high possibility of partial burn. The Nebula shows the lowest levels of HC for all λ-values. Unfortunately, the crevice volume for the Nebula is only 56% compared to the others with squish area because the first piston ring is located higher on that one-piece piston. This is probably the explanation for the Nebula's low HC emissions [7]. The crevice volume for the Flat is 68% compared to the others with squish area because the piston crown is lower on that piston to get the correct compression ratio. The small crevice volume and the smallest piston area compensate the lack of turbulence except when the λ-values are greater than 1.6. Then the increase of HC as a function of λ is greater than average due to a higher amount of partial burn. The Square with large squish areas and the fastest combustion maintains good HC values even for the highest λ-values.

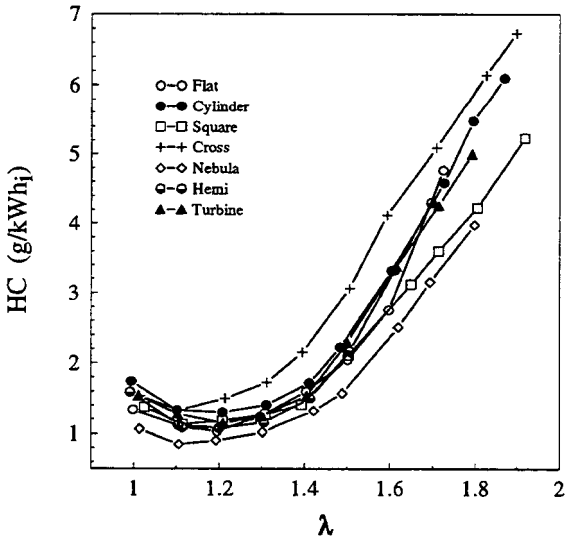

Figure 8: The HC emissions for different combustion chambers. The engine operated at MBT and 1200 rpm.

Figure 9 shows the NO_X emissions for the different combustion chambers. The maximum values at λ=1.2 show that the Square with the fastest combustion has the highest value and the Flat has the lowest. The other combustion chambers show no easily explained pattern.

The NO_X maximum value is very sensitive to ignition timing and a small offset from MBT gives noticeable results. The maximum value is of course of less interest than the NO_X value close to lean limit. Figure 10 shows the NO_X emissions for the different combustion chambers when λ>1.4. The Square and the Cross have the lowest NO_X values because they have the highest lean limit. The Flat and Nebula also show a low minimum level of NO_X.

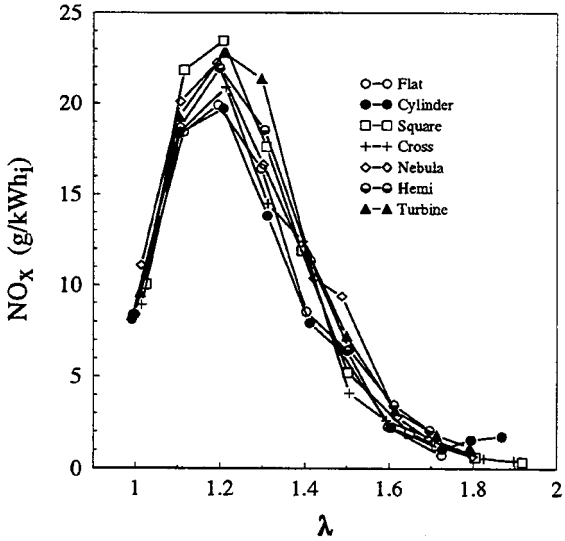

Figure 9: The NO_X emissions for different combustion chambers. The engine operated at MBT and 1200 rpm.

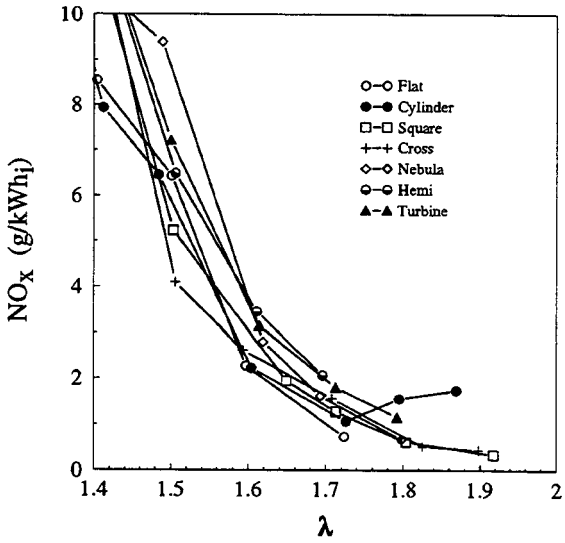

Figure 10: The NO_X emissions for different combustion chambers. The engine operated at MBT and 1200 rpm.

As the sum of HC and NO_X is used as a measure in legislation of emission levels this is shown in figure 11

plotted as a function of λ. This figure indicates that the Nebula and the Square are the best combustion chambers for lean burn.

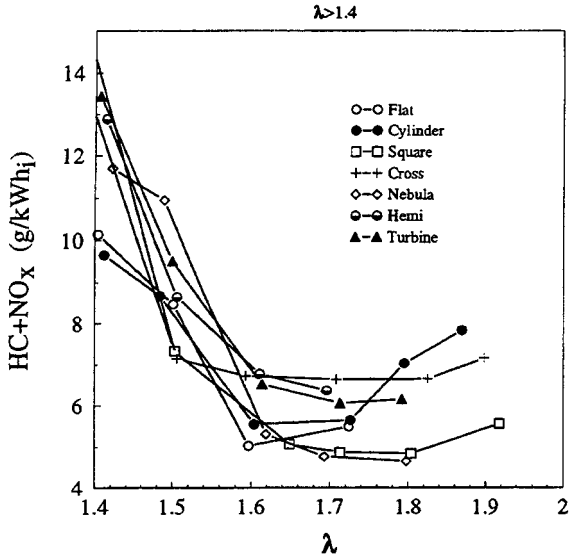

Figure 11: The HC+NO_X emissions for different combustion chambers. The engine operated at MBT and 1200 rpm.

EXHAUST GAS RECYCLED (EGR)

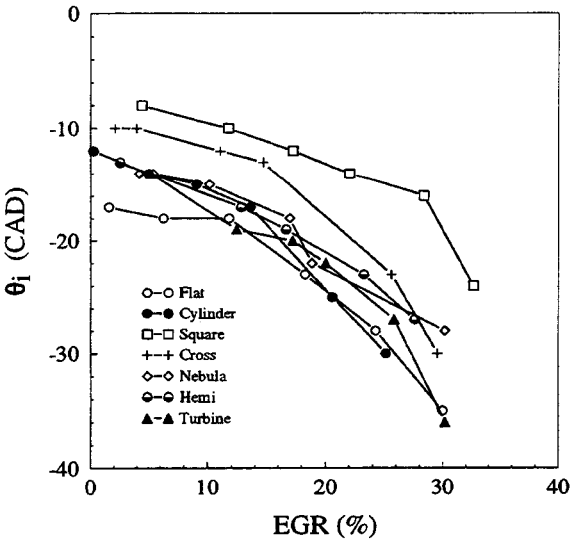

Figure 12: The crank angle position for ignition timing when different combustion chambers are used. The engine operated at MBT and 1200 rpm.

Combustion- Figure 12 above shows the ignition angle θ_i when the engine was run with MBT and with different EGR. The Square combustion chamber has the latest ignition timing for MBT, followed by the Cross. The Flat has the earliest ignition timing.

Figures 13 and 14 show the crank angle for 0 to 10% and 10 to 90% of the total heat released when the engine was run with MBT and with different EGR.

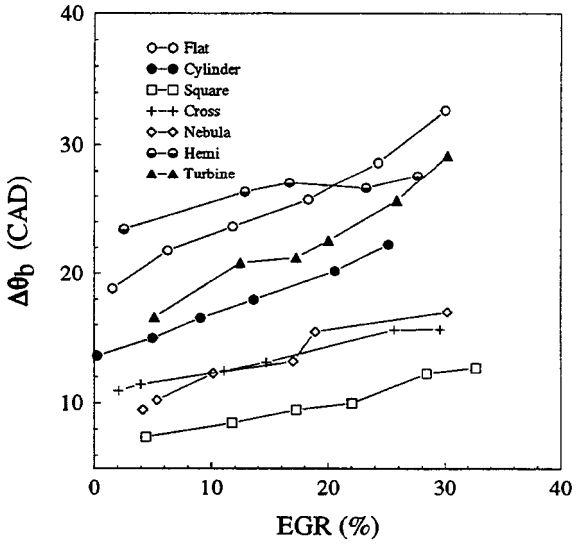

Figure 13: The flame-development angle $\Delta\theta_d$ for 0 to 10% of the total heat released when different combustion chambers are used. The engine operated at MBT and 1200 rpm.

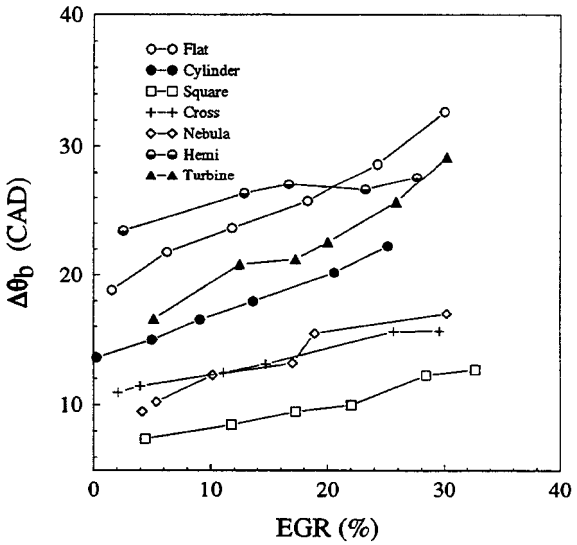

Figure 14: The rapid-burn angle $\Delta\theta_b$ for 10 to 90% of the total heat released when different combustion chambers are used. The engine operated at MBT and 1200 rpm.

As can be seen it is the Square combustion chamber that has the fastest 10 to 90% combustion. The Flat chamber,

with no squish, and the Hemi are clearly the slowest with almost twice as long duration for the combustion.

There are less differences for the 0 to 10% combustion but the combustion chambers follow more or less the same order. These figures look as expected very much like figures 4 and 5 for lean burn.

Figure 14 also shows the EGR limit for the different combustion chambers as the right end point of the curves. The Square has the highest EGR limit and the Cylinder the lowest. This low value for the Cylinder is somewhat surprising but it was rather difficult to obtain stable EGR values over 25% due to the EGR control system and it is possible that the last EGR value without misfire for the Cylinder is somewhat higher than the one in the figure.

Cycle-to-cycle variations- Figure 15 shows the COV_{imep} for the different combustion chambers when the engine was run with MBT and with different EGR. The figure shows that with one exception COV_{imep} is almost the same for the different combustion chambers and is almost constant up to the EGR limit. The Flat combustion chamber with no squish is the only one with a COV_{imep} over 1% without any misfires and this only as a result of partial burn near the EGR limit.

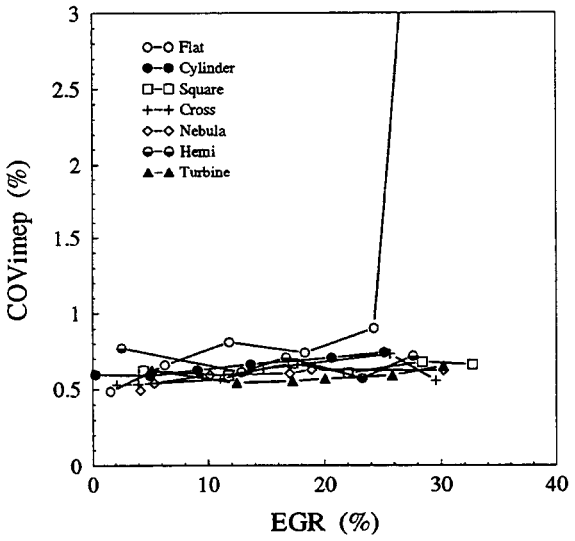

Figure 15: The COV_{imep} for different combustion chambers. The engine operated at MBT and 1200 rpm.

Efficiency- Figure 16 shows the indicated efficiency η_i when the engine was run with MBT and with different EGR. The figure indicates that turbulence generating design features such as large squish areas decrease the efficiency. Compared with lean burn the values for indicated efficiency are lower for EGR and only show a small increase for increasing EGR values.

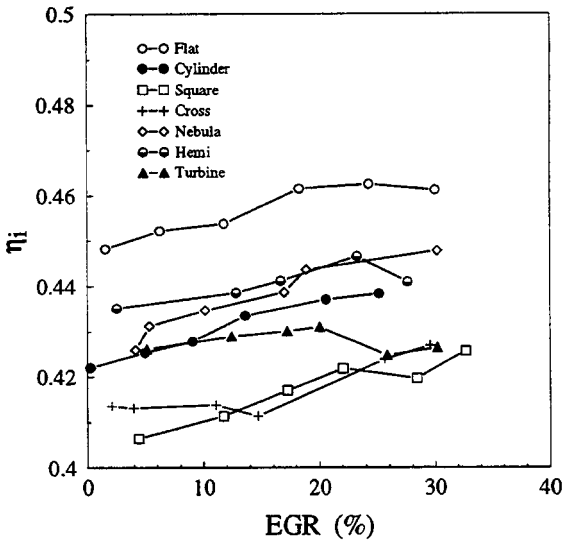

Figure 16: The indicated efficiency η_i for different combustion chambers. The engine operated at MBT and 1200 rpm.

Emissions- Figure 17 shows the HC emissions for the different combustion chambers. The Cross shows the highest levels of HC for all EGR-values as it did for lean burn. The reasons are believed to be the same as for lean burn. The small crevice volume and the smallest piston area for the Flat compensate the lack of turbulence and give this combustion chamber the lowest level of HC emissions. It is interesting to note the much smaller increase in HC when EGR is applied compared to lean burn.

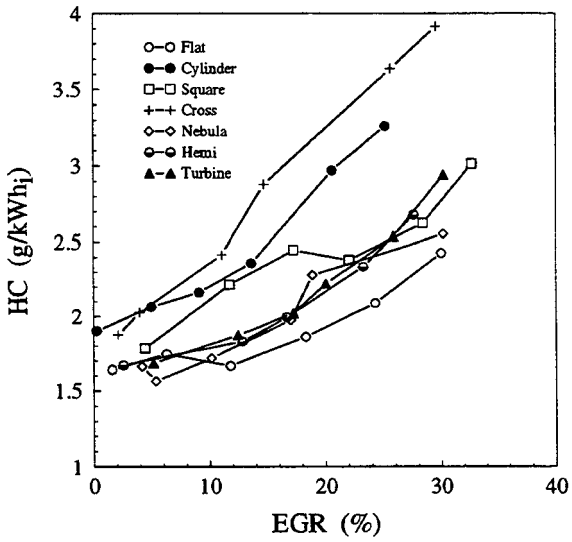

Figure 17: The HC emissions for different combustion chambers. The engine operated at MBT and 1200 rpm.

Figure 18 shows the NO_X emissions for the different combustion chambers. The Cylinder, the Square and the Cross have lowest NO_X values. A possible explanation is that these combustion chambers have the largest residual gas volumes due to the perpendicular walls of the recess in the piston. The same tendencies could be found for medium λ-values in Figure 9 for lean burn.

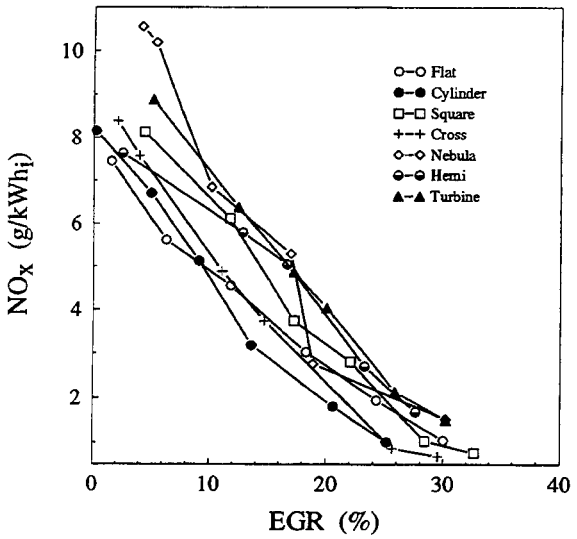

Figure 18: The NO_X emissions for different combustion chambers. The engine operated at MBT and 1200 rpm.

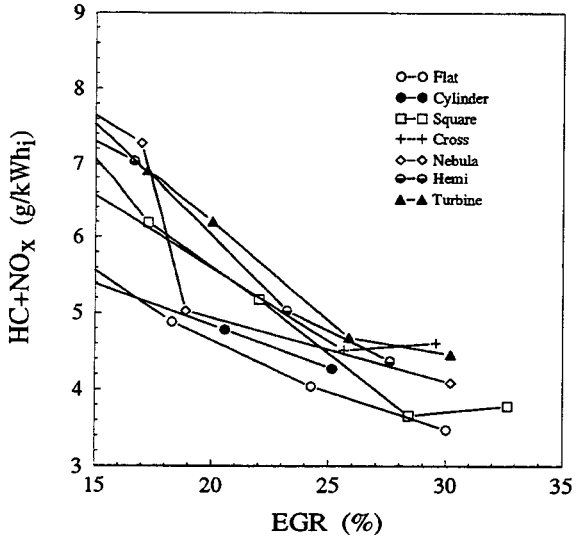

Figure 19: The HC+NO_X emissions for different combustion chambers. The engine operated at MBT and 1200 rpm.

As the sum of HC and NO_X is used as a measure in legislation of emission levels this is plotted as a function of EGR in figure 19. This figure indicates that the Flat is the best combustion chamber for EGR. This is mainly due to the low HC emissions from the small crevice volume.

CORRELATIONS

Emissions and compression ratio- NO_X emissions and compression ratio showed no correlation for the tested geometries. However this was not expected [8].

Increasing compression ratio increases the HC emissions. Figure 20 shows the HC emissions as a function of compression ratio for different combustion chambers for λ=1.8.

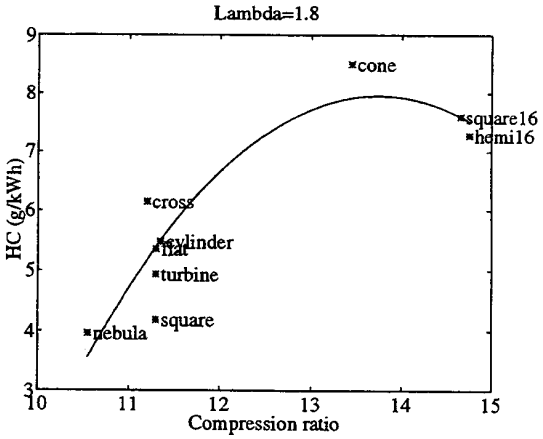

Figure 20: HC emissions as a function of compression ratio for different combustion chambers. The engine operated at MBT and 1200 rpm.

Several factors could contribute: increased importance of crevice volumes at high compression ratio, lower gas temperatures during the latter part of the expansion stroke, thus producing less HC oxidation in the cylinder; lower exhaust temperatures, and hence less oxidation in the exhaust system [8].

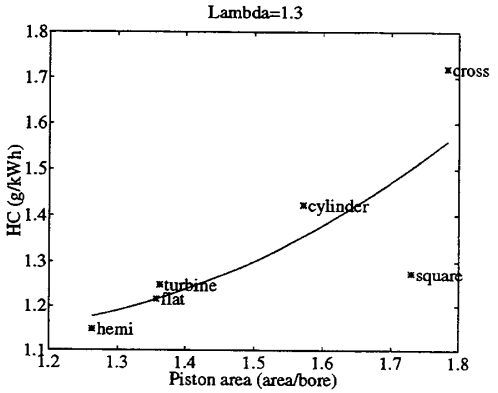

Figure 21: HC emissions as a function of relative piston area for different combustion chambers. The engine operated at MBT and 1200 rpm.

Piston area and HC emissions- A correlation can be found between piston area and HC emissions for the different combustion chambers but only at λ=1.3 when the HC emissions are low. Then the effect of wall quenching is dominating and no bulk quenching due to partial burn is likely to appear. Figure 21 above shows the HC emissions as a function of relative piston area (piston area/bore area) for different combustion chambers for λ=1.3.

Piston area and NO_x emissions- A correlation can be found between piston area and NO_x emissions for the different combustion chambers. Figure 22 shows the NO_x emissions as a function of relative piston area for different combustion chambers for λ=1.5.

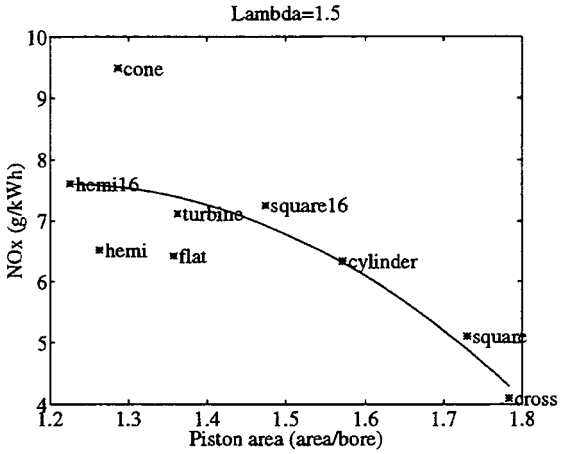

Figure 22: NO_x emissions as a function of relative piston area for different combustion chambers. The engine operated at MBT and 1200 rpm.

DISCUSSION

Is it now possible to choose the best strategy, lean burn or EGR, and the best combustion chamber from the presented results? The choice depends on if emissions or efficiency or a mixture of both are the objectives to meet [10]. In figure 23 below $HC+NO_x$ is plotted as a function of indicated efficiency for the different combustion chambers and for λ>1.4. The information from the figure is that the low emission values for the Square are combined with a rather low efficiency and it is best to choose between the Flat and the Nebula. All emissions that have been measured are raw emissions. If a hypothetical oxidation catalyst with a 70% reduction of HC emissions is added the possible result is shown in figure 24. With this hypothetical catalyst the lowest emissions are obtained with the Square and the Nebula. The efficiency of the Nebula is however superior and is thus the recommended choice.

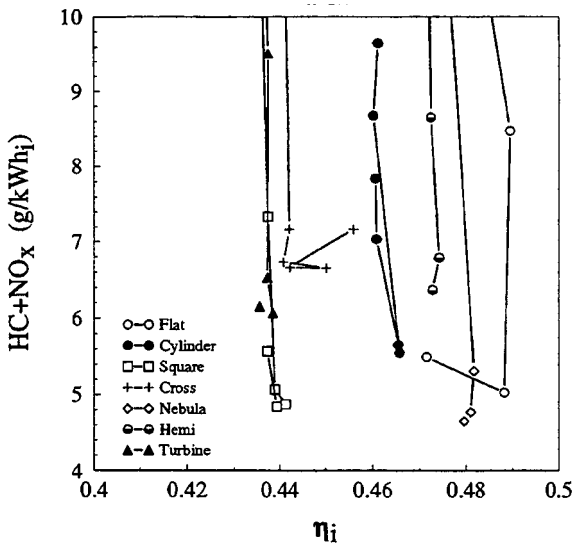

Figure 23: The $HC+NO_x$ emissions as a function of indicated efficiency for different combustion chambers and # values. The engine operated at MBT and 1200 rpm.

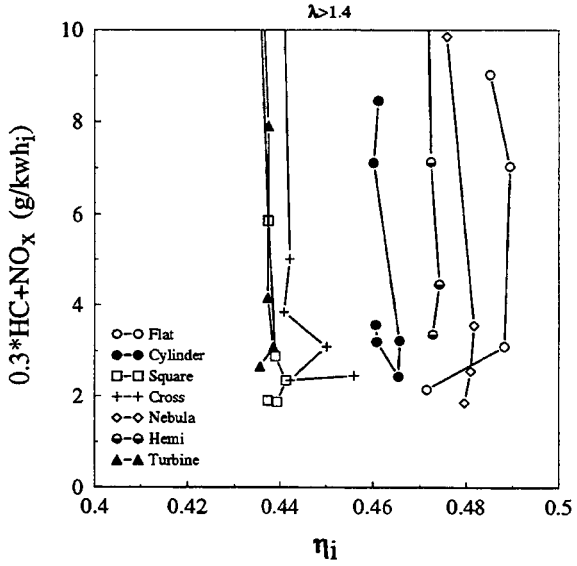

Figure 24: The $0.3*HC+NO_x$ emissions as a function of indicated efficiency for different combustion chambers and # values. The engine operated at MBT and 1200 rpm.

The same figures for different EGR values are found below. In this case the hypothetical catalyst is a three-way catalyst with a 75% reduction of HC emissions and a 90% reduction of NO_x emissions.

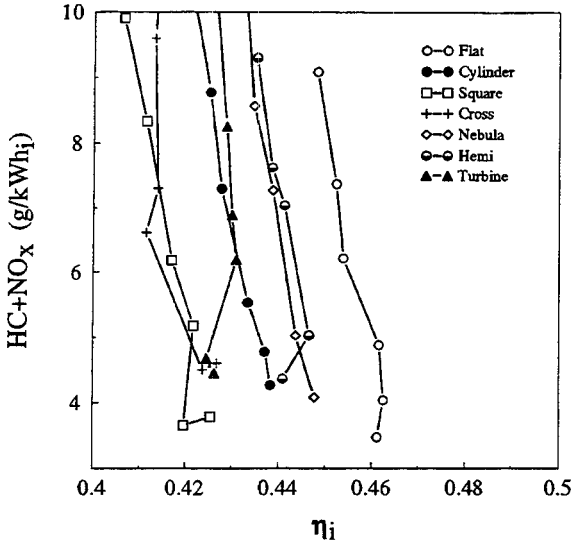

Figure 25: The HC+NO_x emissions as a function of indicated efficiency for different combustion chambers and EGR values. The engine operated at MBT and 1200 rpm.

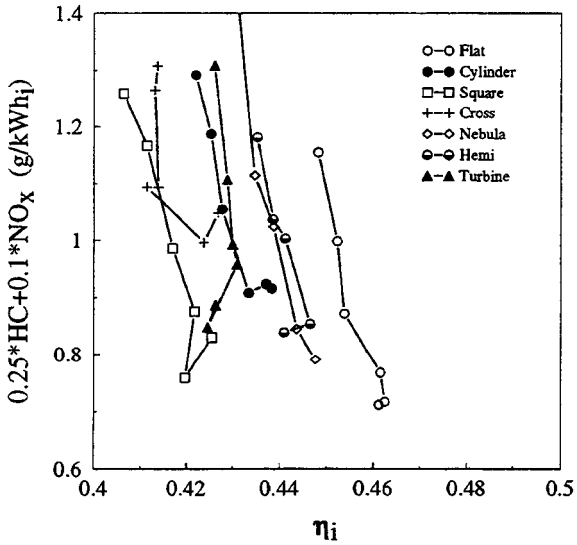

*Figure 26: The 0.25*HC+0.1*NO_x emissions as a function of indicated efficiency for different combustion chambers and EGR values. The engine operated at MBT and 1200 rpm.*

The increase from 70% to 75% reduction of the HC emissions is justified by the increased exhaust temperature of EGR operation. The information from the figures shows that it is best to choose the Flat combustion chamber. This is somewhat surprising. Aside from the small crevice volume for the Flat combustion chamber, a possible explanation for this result is that the definitions of lean limit and EGR limit never give the turbulence generating designs a chance to prove that they can extend lean limit and EGR limit compared to the Flat. But in the future HC emissions can not be neglected and a lean limit defined at 5% COV_{imep} [1],[2],[9] is likely to produce too much HC emissions.

EGR combined with a three-way catalyst shows the lowest emission values at the price of a lower efficiency than lean burn.

CONCLUSIONS

1. Regardless of combustion chamber design λ=1.0 plus EGR gives somewhat better total (HC+NO_x) emissions, but with a lower efficiency, than lean burn.

2. Combined with a three-way catalyst λ=1.0 plus EGR shows a potential for really low total emission values that are not possible to achieve with lean burn and an oxidising catalyst.

3. The Square combustion chamber which has the fastest combustion has the lowest NO_x emissions at lean burn.

4. If no misfire is accepted the Flat combustion chamber and the Nebula combustion chamber show the lowest total emissions together with the best efficiencies.

REFERENCES

[1] T. Naganuma, M. Iko, T. Sakonji, F. Shoji: "Basic Research on Combustion Chambers for Lean Burn Gas Engines" 1992 Int. Gas Research Conference.

[2] T. Sakurai, M. Iko, K. Okamoto, F. Shoji: "Basic Research on Combustion Chambers for Lean Burn Gas Engines" SAE932710

[3] W.R. Dietrich, W. Grundmann, G. Langeloth: "Pollutant Reduction on Stationary S.I. Engines from Motoren-Werke Mannheim for Operation on Natural Gas Applying the Lean-Burn Principle" (In German) MTZ, Motortechniche Zeitschrift 47(1986) 3 pp83-87

[4] J Nilsson: "A Study on a Low Emission Combustor - Lean Premix Prevaporize Concept" Licenciate Thesis ISRN LUTMDN/TMVK--7014-SE Dept. of Heat & Power Engineering, Lund Inst. of Techn. 1993.

[5] B. Johansson: "Correlation Between Velocity Parameters Measured with Cycle-Resolved 2-D LDV and Early Combustion in a Spark Ignition Engine" Licenciate Thesis ISRN LUTMDN/TMVK --7012-SE Dept. of Heat & Power Engineering, Lund Inst. of Techn. 1993

[6] G. Woschni: "A Universally Applicable Equation for Instantaneous Heat Transfer Coefficient in the Internal Combustion Engine" SAE670931

[7] H. Carstensen:
"Systematische Untersuchung der Konstruktions- und Betriebsparameter eines Zweiventilmagermotors auf Kraftstoffverbrauch, Schadstoffemission und Maximalleistung" Dissertation TUW 1991 Vortschrittberichte VDI Reihe 12 Nr 163

[8] J. B. Heywood:
"Internal Combustion Engine Fundamentals" ISBN 0-07-100499-8 p844.

[9] M.G. Kingston Jones, M.D. Heaton:
"Nebula Combustion System for Lean Burn Spark Ignited Gas Engines"
SAE890211

[10] Y. Nakajima, K Sugihara and Y. Takagi:
"Lean Mixture or EGR - Which is better for Fuel Economy and NO_x Reduction?"
I Mech E Conference Publication C94/79 1979.